VesselJ: A New Tool for Semiautomatic Measurement of Corneal Neovascularization

Alessandro Rabiolo, Fabio Bignami, Paolo Rama, and Giulio Ferrari

Cornea and Ocular Surface Unit, Eye Repair Lab, IRCCS San Raffaele Scientific Institute, Milan, Italy

Correspondence: Giulio Ferrari, Cornea and Ocular Surface Unit, Eye Repair Lab, (Istituto di Ricovero e Cura a Carattere Scientifico) IRCCS San Raffaele Scientific Institute, Via Olgettina 60, 20132 Milan, Italy; ferrari.giulio@hsr.it.

Submitted: April 14, 2015
Accepted: November 4, 2015

Citation: Rabiolo A, Bignami F, Rama P, Ferrari G. VesselJ: a new tool for semiautomatic measurement of corneal neovascularization. *Invest Ophthalmol Vis Sci*. 2015;56:8199–8206. DOI:10.1167/iovs.15-17098

Purpose. To quantify blood and lymph angiogenesis in mouse corneal flat mounts by means of a novel plug-in for ImageJ, called VesselJ, based on a dynamic threshold algorithm.

Methods. Corneal neovascularization (CNV) was induced in the right corneas of 20 C57BL6/N mice by means of alkali burn ($n = 10$) or intrastromal sutures ($n = 10$). All corneal flat mounts were stained for blood vessels with CD31 and for lymphatics with LYVE1. Three independent operators measured blood and lymphatic CNV with both a published manual method (mCNV) and VesselJ (automatic method; aCNV).

Results. Both methods showed a strong reliability, defined as intraclass correlation coefficient (ICC) > 0.90, in quantifying hemangiogenesis for sutures and alkali burn. However, reliability of lymphatic mCNV varied from moderate in alkali burn (ICC: 0.700) to poor in sutures (ICC: 0.415), whereas it remained high in aCNV (alkali ICC: 0.996; sutures ICC: 0.959). Among sutures, a significant correlation between mCNV and aCNV was found among all the three operators for blood vessels and just for one operator for lymphatic vessels ($P < 0.001$). In the alkali burn model, correlation between blood mCNV and aCNV was significant for all operators after excluding three noisy flat mounts ($P < 0.001$), whereas no significant correlation was seen for lymphatic vessels.

Conclusions. VesselJ is a semiautomatic, reliable, and fast method to quantify corneal hem- and lymphangiogenesis in corneal flat mounts. VesselJ can be easily used in the sutures model; it should be applied to other models (e.g., alkali burn) only after checking for background hyperfluorescence.

Keywords: corneal neovascularization, blood vessels, lymphatics, plug-in, ImageJ

Scopo. Quantificare l'angiogenesi e la linfangiogenesi su cornee murine tramite un nuovo plugin per ImageJ, chiamato VesselJ, basato su un algoritmo dinamico per la determinazione di un valore soglia.

Metodi. La neovascolarizzazione corneale (CNV) è stata indotta nella cornea destra di 20 topi C57BL6/N tramite ustione da alcali (n = 10) o applicazione di suture intrastromali (n = 10). Le cornee sono state marcate per i vasi sanguigni con CD31 e per i linfatici con LYVE1. Tre operatori indipendenti hanno misurato la CNV ematica e linfatica con un metodo manuale precedentemente pubblicato (mCNV) e con VesselJ (aCNV).

Risultati. Entrambi i metodi hanno mostrato una forte riproducibilità, definita da valori di Coefficiente di Correlazione Intraclasse (ICC) > 0.90, nel quantificare l'angiogenesi in entrambi i modelli. Tuttavia, la riproducibilità del mCNV linfatico variava da moderata nell'ustione da alcali (ICC: 0.700) a scarsa nelle suture (ICC:0.415), mentre rimaneva sempre alta nell'aCNV (ICC alcali: 0.996; ICC suture: 0.959). Riguardo il modello suture, è stata osservata una correlazione significativa tra mCNV e aCNV per tutti gli operatori riguardo i vasi ematici e per solo un operatore per i vasi linfatici ($P < 0.001$). Nel modello dell'ustione è stata osservata una correlazione significativa tra mCNV e aCNV ematici per tutti gli operatori dopo aver escluso 3 immagini con elevato rapporto segnale/rumore ($P < 0.001$), viceversa nessuna correlazione significativa è stata osservata per i vasi linfatici.

Conclusioni. VesselJ è un metodo semi-automatico, preciso e rapido per quantificare angiogenesi e linfangiogenesi su cornee murine. VesselJ può essere agevolmente impiegato nel modello suture, ma dovrebbe essere applicato ad altri modelli (es. ustione da alcali) solo dopo aver controllato l'iperfluorescenza di fondo.

Investigative Ophthalmology & Visual Science

The cornea is the outer dome covering the eye anteriorly, and its transparence is key to allow proper vision. Total absence of blood and lymphatic vessels in the normal cornea, known as "angiogenic privilege,"[1] is required to maintain a transparent cornea.

Corneal neovascularization (CNV) occurs in many sight-threatening conditions, such as infectious keratitis, ocular pemphigoid, and Stevens-Johnson syndrome, among others.[2]

Animal models of CNV are outstanding models to observe the sprouting of blood and lymphatic vessels and to test pro- or antiangiogenic therapies well beyond ophthalmology, such as in cancer.[3,4] This is due to the easy accessibility of the cornea, which makes both induction and inspection of CNV extremely easy. The gold standard for studying and quantifying blood angiogenesis and lymphangiogenesis ex vivo is to (1) induce CNV; (2) remove and stain the corneas for markers of blood (e.g., CD31) and lymphatic (e.g., LYVE1) vessels, respectively; and (3) quantify the extension of vessels on microscopic images/montages.

Despite technology developments, several studies, even recent ones, use manual methods to estimate CNV. Commonly used manual techniques include grading scales, where a score is arbitrarily given depending on the number, density, and tortuosity of vessels[5–8]; and quantitative methods, where vessel arcades are connected on the inner side and the region from this line and the limbal arcade, normalized for the corneal area, is calculated.[9–12]

Bock et al.[13] described a semiautomatic quantitative method to calculate CNV in corneal flat mounts. This technique resulted in more precision, accuracy, and reproducibility and saved time compared to a manual quantitative method.[13] However, it had several limitations, including the fact that the operator had to manually choose a threshold value for each image, leading to variability and time consumption. Other semiautomatic morphometric techniques have been applied to estimate CNV, although the specific methodology used is not always described.[14–17]

Our work aimed to develop an open-source, user-friendly, downloadable, semiautomatic quantitative plug-in to calculate blood and lymphatic vessels in corneal flat mounts and to compare it to the widely used manual quantitative method.

Methods

Animals

Male, 6- to 8-week-old, C57BL6/N mice (Charles-River, Calco, Italy) were used in all experiments (20 total mice). Animals were allowed to acclimatize for 1 week prior to experimentation. Each animal was deeply anesthetized with intraperitoneal injection of tribromoethanol (250 mg/kg) before all surgical procedures. Postoperatively, all animals received a single dose of carprofen at 5 mg/kg subcutaneous. Carbon dioxide inhalation and subsequent cervical dislocation were applied to euthanize the animals. All experimental protocols were approved by the Animal Care and Use Committee of the IRCCS San Raffaele Scientific Institute, in accordance with the ARVO Statement for the Use of Animals in Ophthalmic and Vision Research.

Corneal Alkali Burn Model

A corneal alkali burn was created in the right eye of 10 mice by means of a paper disc (3-mm diameter) soaked in 1 N NaOH for 10 seconds under slit-lamp examination. The ocular surface was then washed with 15 mL normal saline. To increase reproducibility, a single investigator induced the alkali burn in all animals. On day 14, corneas were removed for immunostaining.

Corneal Suture Placement

Three 10–0 nylon sutures (Alcon Laboratories, Inc., Fort Worth, TX, USA) were placed intrastromally in the right eye of 10 mice, at the 2, 6, and 10 o'clock positions of the cornea, 1 mm away from the limbal vessel, following a demarcation of a 2-mm trephine. To increase reproducibility, a single investigator placed sutures in all animals. On day 10, corneas were collected for immunostaining.

Immunostaining of Corneal Neovascularization

On day 10 or 14, corneas were carefully dissected and rinsed in PBS. The corneal epithelium was subsequently scraped off after ethylenediaminetetraacetic acid (EDTA; Sigma-Aldrich Corp., St. Louis, MO, USA) treatment for 30 minutes at 37°C. Fixation of the tissue was conducted with iced acetone for 15 minutes following 2 hours of blocking in PBS/2%BSA. For visualization of blood and lymphatic vessels, corneas were immunostained with rat anti-mouse CD31 (1:200) 0.5 mg/mL (BioLegend, San Diego, CA, USA) and goat anti-mouse LYVE-1 (1:200) 1 mg/mL (Abcam, Cambridge, UK) at 4°C overnight, respectively, and subsequently with Alexa Fluor-594 donkey anti-rat IgG 2 mg/mL and Alexa Fluor-488 donkey anti-goat IgG 2 mg/mL (Invitrogen-Moleular Probes, Paisley, UK) in a 1:500 dilution for 2 hours at room temperature. This was followed by three rinses in PBS. Corneas were flat mounted on glass slides using Vectashield (Vector Laboratories, Burlingame, CA, USA) mounting medium with 4′,6-diamidino-2-phenylindole (DAPI). The present work was performed in accordance with the Consensus Statement on Immuhistochemical Detection of Ocular Lymphatic Vessels proposed by Schroedl et al.[18]

Assessments of Corneal Neovascularization Ex Vivo

The fluorescence of the vessels was captured using a DFC310FX digital camera (Leica Microsystems, Inc., Wetzlar, Germany), attached to a Leica CTR5500 fluorescence microscope (Leica Microsystems, Inc.) controlled by LAS 3.7.0 software (Leica Microsystems, Inc.). Instrument settings were identical for all the experiments (i.e., exposure, gain, gamma, and saturation). A set of six adjacent, overlapping images was acquired using a ×5 objective with 1392 × 1040 pixels of resolution and saved as 8-bit RGB .tiff format files. Although ×5 magnification potentially results in less detailed images than ×10 magnification, it was used in order to reduce the image acquisition time, together with the bleaching caused by light source overexposure. Images were remapped into a montage, obtaining a two-dimensional reconstruction of the whole cornea by Adobe Photoshop CS5 12.0 (Adobe Systems, San Jose, CA, USA).

Manual Assessment. Digital pictures of the flat-mounted corneas were analyzed through ImageJ 1.48p software (National Institutes of Health, Bethesda, MD, USA). The total area of the cornea was encircled by drawing a freehand region with the ImageJ command Polygon Selections, outlining the innermost vessels of the limbal arcade. The area outside the total corneal area was erased and substituted with white color using the ImageJ command Clear Outside from the Edit menu. Vessel sprouts were connected using a freehand selection. Manual CNV (mCNV) was calculated as the difference between the total corneal area and the avascular area, normalized for the total corneal area.[6] Figure 1 shows key passages to manual quantifying both blood and lymphatic vessels in corneal flat

Investigative Ophthalmology & Visual Science

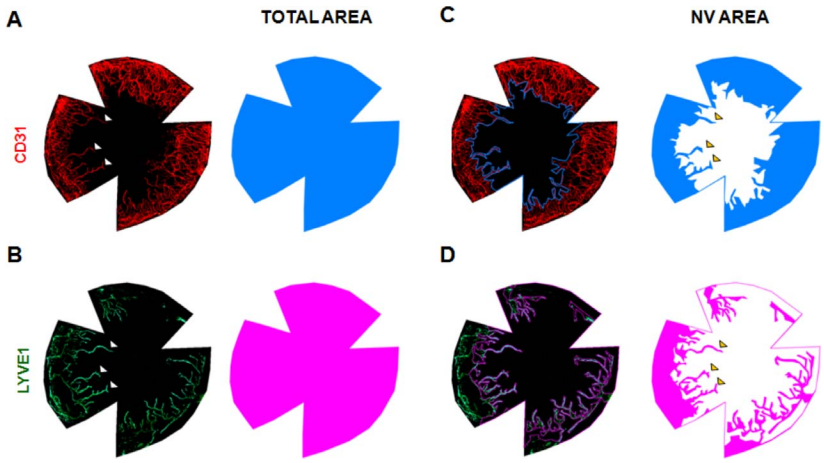

FIGURE 1. Key passages to manually quantify blood and lymphatic angiogenesis. (**A**, **B**) Firstly, total corneal area was delineated and calculated for blood vessels (*red*) and lymphatics (*green*), here represented in *blue* and *violet areas*, respectively. (**C**, **D**) Secondly, blood and lymphatic vessel arcades were connected on the inner side (*blue* and *violet lines*, respectively). The neovascular (NV) area is between this line and the limbal arcade (*blue* and *violet* selection). Manual corneal neovascularization (mCNV) was calculated as the ratio between NV area and total corneal area. *Arrows* show that lymphatics are positive for both CD31 and LYVE1 markers.

mounts. Four manual analyses were performed: blood and lymphatic CNV measures for the alkali burn and sutures models. Each analysis was repeated by three different operators. All images from the sutures group were analyzed three times by each operator at 0, 2, and 3 months.

Automated Assessment. A new homemade plug-in for the freeware software ImageJ, called VesselJ (soon available in the public domain, http://imagej.nih.gov/ij/plugins/index.html), was developed to assess the corneal hemangiogenesis and lymphangiogenesis on digital pictures in an automatic way. VesselJ was written in Batch language adapted for ImageJ. The white background was automatically excluded by skipping pixels with RGB value of 255.255.255. The automatic analysis relied on a corneal background-adjusted threshold, based on the red channel for blood vessels and on the green channel for lymphatic vessels. Four automatic analyses were performed: blood and lymphatic CNV measures for the alkali burn and sutures models. Each analysis was repeated by three different operators. All images from the sutures group were analyzed three times by each operator at 0, 2, and 3 months. A detailed step-by-step protocol used to process images with the VesselJ plug-in is provided below, and a demonstrative video is provided in the Supplementary Material.

VesselJ Algorithm

The operator launched the plug-in once for each analysis. Ten images with the total area defined as described in the paragraph on manual assessment were simultaneously opened. No changes in the pictures' brightness, colors, balance, or contrast were made. The operator was instructed to choose a rectangular area of the corneal background, called region of interest (ROI), for each image. The operator was advised to include autofluorescence within the background ROI, but to ensure that it was free from vessels and hyperfluorescent artifacts (Supplementary Fig. S1). The ROI value was autonomously determined by each operator, depending on the background pattern of each single image. The operator was instructed not to put the ROI box in an area totally free of autofluorescence and artifacts, as this would negatively affect the background-adjusted threshold determination. From this step onward, VesselJ processed images automatically, and no additional operator input was needed. VesselJ calculated the red and green color mean values within the background ROI for CD31- and LYVE1-labeled images, respectively. Since color values were normalized for total selected area, ROI size did not significantly affect the computation. In order to confirm that image analysis does not depend on ROI size, one operator (AR) analyzed all the images using three different ROI sizes: small (60×32 pixels), medium (112×72 pixels), and large (188×156 pixels). In our setting, the plug-in used red pixels to analyze the $CD31^+$ blood vessels and green pixels to analyze $LYVE1^+$ lymphatic vessels. Depending on the mean redness or "greenness," a different stepwise threshold value was automatically set for that image. Threshold values vary from lymphatic to blood vessels. First, white pixels (RGB 255.255.255) were excluded from the analysis because they represent the white background surrounding corneal images. Pixels above the threshold value were counted as neovessels, while pixels below the threshold were counted as nonvascularized pixels. Total pixels of the cornea were calculated as neovascularized plus nonvascularized pixels. The automatic CNV (aCNV) was calculated as the ratio between the neovascularized pixels and the total pixels of the cornea. Vascularized and nonvascularized areas were expressed as pixels, while the aCNV was a dimensionless number. Once VesselJ completed the analysis of the last picture of the group, title and data of each image were shown in a separate window and exported to an Excel file (Microsoft Corp., Redmond, WA, USA). Figure 2 shows key passages needed to quantify both blood and lymphatic vessels in corneal flat mounts with VesselJ.

Statistics

Interobserver reliability of aCNV and aCNV index assessed by different operators was calculated using intraclass correlation coefficient (ICC). Systemic differences among operators over time were evaluated with repeated measures ANOVA. Comparison between the results of automated and manual assessments was performed using Pearson correlations. Time analysis was performed using one-way ANOVA following Bonferroni post hoc tests. Significance was defined as a P value < 0.05. All results are presented as mean $\pm$ standard deviation (SD). All statistics were performed using GraphPad Prism software 5.0 (GraphPad Software, Inc., San Diego, CA, USA) and SPSS software 21 (SPSS, Inc., Chicago, IL, USA). Data

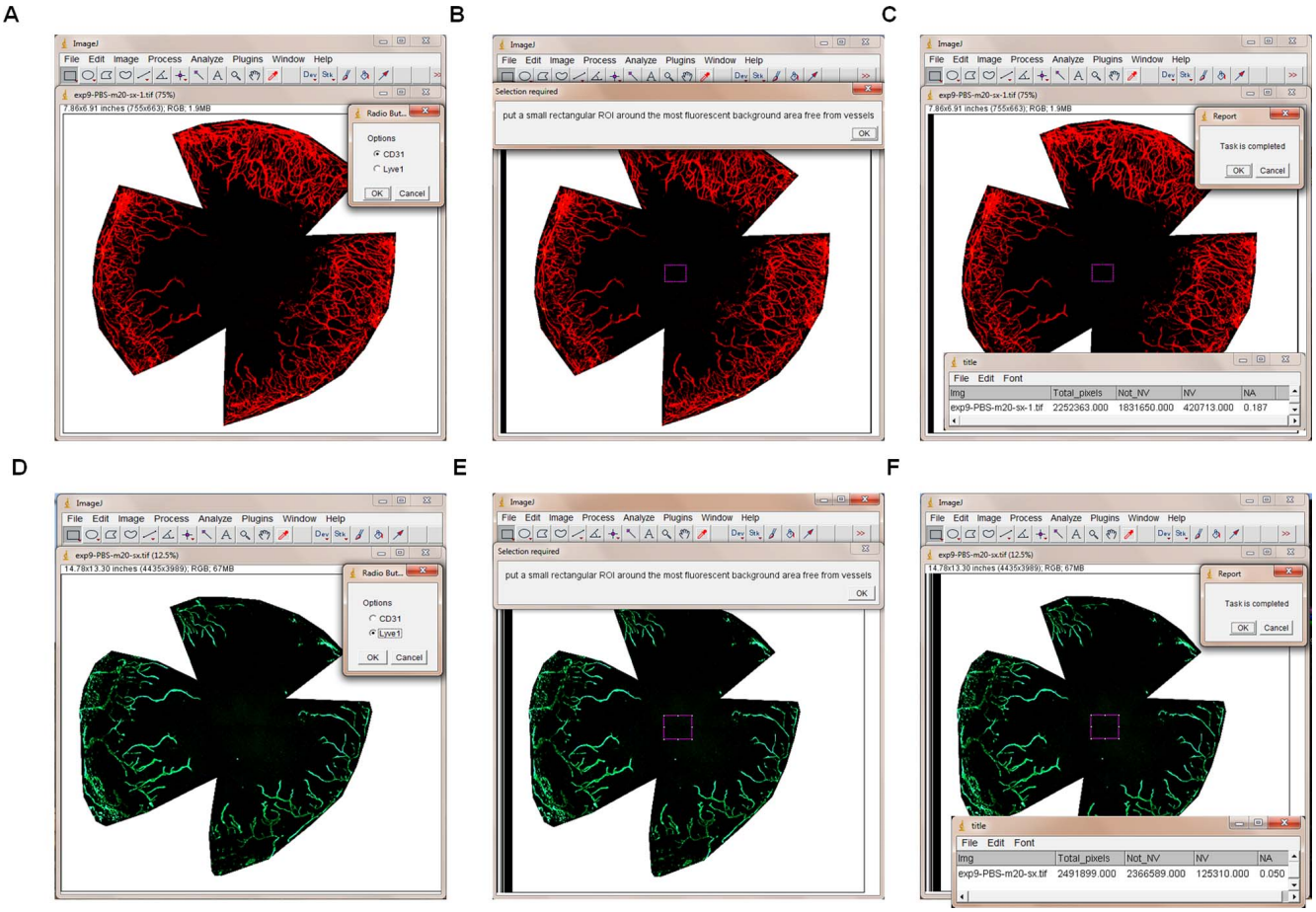

Figure 2. Screenshot of VesselJ interface during blood and lymphatic vessel quantification. Key passages are illustrated: (**A**, **D**) choosing the marker (i.e., CD31 or LYVE1); (**B**, **E**) selection of background region of interest (ROI); (**C**, **F**) an alert box communicating that VesselJ finished analyzed images; results are displayed in a separate window.

presentation adheres to guidelines for reporting reliability and agreement studies proposed by Kotnner et al.[19]

Results

Forty flat-mount corneal images were analyzed in this study. Images were split into four groups of 10 pictures each, depending on the model of CNV used (alkali burn versus sutures) and on vessel type (blood versus lymphatic vessels). Three independent and trained operators analyzed all the images. Figure 3 shows pooled mCNV and aCNV values.

It has been already shown that both alkali burn and sutures models induce more blood than lymphatic CNV, although CD31 stains both. The sutures model is more reproducible in inducing CNV than the alkali burn model. Even though the alkali-burned and sutured corneas were harvested at different times, the SD from the mean of blood and lymphatic mCNV in the alkali model was higher than that obtained in the sutures model (0.11 vs. 0.06 for blood mCNV; 0.13 vs. 0.05 for lymphatic mCNV).

ROI Size Analysis

As shown in Supplementary Figure S2, all the aCNV values were identical for both the alkali burn and sutures models for blood vessels regardless the ROI size. With regard to the lymphatic vessels, only one cornea (out of 10) had a different aCNV value in both models, albeit these differences were not significant either in the alkali burn ($P = 0.3874$, ANOVA for repeated measures) or in the sutures ($P = 0.384$, ANOVA for repeated measures) model.

Intra- and Interoperator Concordance for Manual and Automatic Quantification

Interoperator reliability for both manual and automatic method is shown in Table 1. With regard to blood mCNV, a strong reliability (ICC > 0.90) for both sutures (0.916) and alkali burn (0.972) was observed. In particular, the measure of blood mCNV showed a higher confidence interval (CI 95%) in the alkali burn model (0.923–0.992) compared to the sutures (0.756–0.977).

Reliability of manually assessed lymphatic vessels varied from moderate (ICC = 0.700) in the alkali burn model to poor (ICC = 0.415) in sutures, with a wider CI (0.245–0.913, for alkali burn; 0.063–0.769, for sutures) than for blood mCNV.

By contrast, aCNV interoperator reliability was very strong in all four groups, with an ICC higher than 0.959 (CI 0.889–1.00).

With regard to the sutures model, the manual method showed highly systemic variability for all operators both for blood ($P < 0.0001$, $P = 0.0008$, $P < 0.0001$ for operators 1, 2, and 3, respectively) and lymphatic ($P = 0.0078$, $P < 0.0001$, P

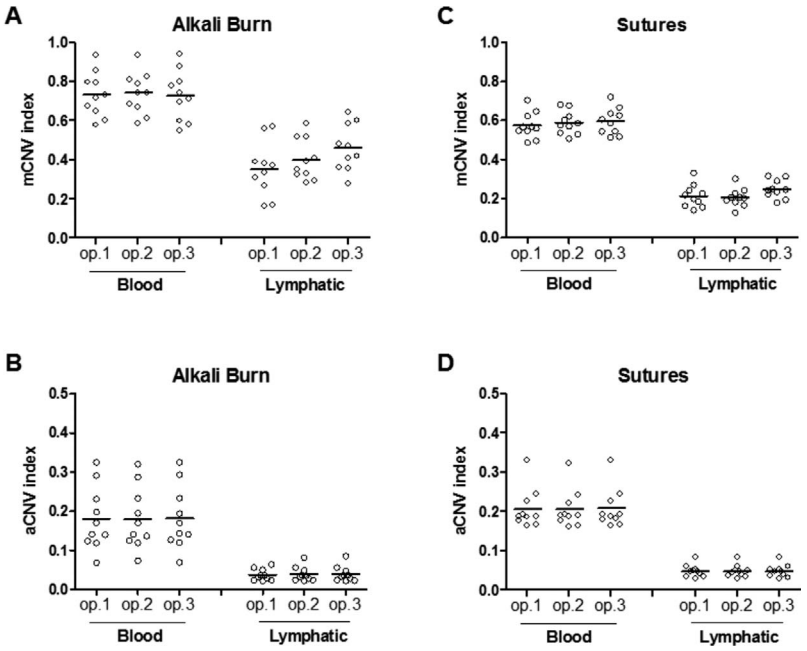

FIGURE 3. Corneal neovascularization values among all three operators. Manual corneal neovascularization (mCNV) and automatic corneal neovascularization (aCNV) indexes in alkali burn (**A**, **B**, respectively) and sutures (**C**, **D**, respectively) models for all three operators. Op. 1, 2, and 3 stand for operators 1, 2, and 3 ($n = 10$).

= 0.0047 for operators 1, 2, and 3, respectively) vessels. Conversely, all operators exhibited identical results for blood vessels and no significant systemic differences for lymphatic vessels ($P = 0.3874$, $P = 0.1545$, $P = 0.1372$ for operators 1, 2, and 3, respectively) using VesselJ (data not shown).

Concordance Between Manual and Automatic Quantification

Correlations between mCNV and aCNV quantifications for each operator are shown in Table 2. With regard to the sutures model, a significant correlation was found among all operators for blood vessels ($P = 9.01E\text{-}05$, $P = 6.48E\text{-}03$, $P = 1.10E\text{-}03$ for operators 1, 2, and 3, respectively), whereas just one out of three operator (operator 2) exhibited a significant correlation for lymphatic vessels between the mCNV and aCNV analysis (Pearson $r = 0.893$, $P = 4.98E\text{-}04$), as shown in Figure 4.

In the alkali burn model, no significant correlation was found between mCNV and aCNV for both blood and lymphatic vessels. However, 3 images out of 10 and 6 out of 10 for blood and lymphatic vessels, respectively, showed an intense autofluorescent background and/or massive hyperfluorescent cellular infiltration (Supplementary Fig. S3). By excluding from the analysis these three noisy flat mounts, a significant correlation was found between blood mCNV and aCNV for all the operators, as shown in Table 2 ($P = 1.35E\text{-}03$, $P = 1.45E\text{-}03$, $P = 6.77E\text{-}03$ for operators 1, 2, and 3, respectively).

TABLE 1. Concordance Among Operators

Corneal Model	Angiogenesis	ICC (CI 95%)
Manual method		
Sutures	Blood	0.916 (0.756–0.977)
Sutures	Lymphatic	0.415 (0.063–0.769)
Alkali burn	Blood	0.972 (0.923–0.992)
Alkali burn	Lymphatic	0.700 (0.245–0.913)
Automatic method		
Sutures	Blood	0.998 (0.994–0.999)
Sutures	Lymphatic	0.996 (0.988–0.999)
Alkali burn	Blood	0.999 (0.998–1.000)
Alkali burn	Lymphatic	0.959 (0.889–0.989)

Time Analysis

The amount of time needed to analyze images with VesselJ was significantly reduced in the automated versus manual system in the alkali burn model (Fig. 5). Specifically, mean times of the three operators to calculate lymphatic vessels per image ($n = 10$) were 546.7 ± 165.2 seconds and 25.5 ± 2.8 seconds for the manual method and VesselJ, respectively ($P < 0.001$). For blood vessels, 148.5 ± 20.8 and 25.5 ± 2.3 seconds was spent by each operator for each image ($n = 10$) with the manual method and VesselJ, respectively ($P < 0.001$). No difference of time was seen for automatic blood and lymphatic quantifica-

TABLE 2. Concordance Between Manual and Automatic

Corneal Model	Operator	N	Pearson r	P Value
Blood vessels				
Sutures	1	10	0.931	9.01E-05
Sutures	2	10	0.791	6.48E-0.3
Sutures	3	10	0.869	1.10E-0.3
Alkali burn	1	7	0.858	1.35E-0.3
Alkali burn	2	7	0.854	1.45E-0.3
Alkali burn	3	7	0.893	6.77E-0.4
Lymphatic vessels				
Sutures	1	10	0.504	1.37E-01
Sutures	2	10	0.893	4.98E-04
Sutures	3	10	0.430	2.15E-01
Alkali burn	1	10	−0.178	6.23E-01
Alkali burn	2	10	−0.251	4.84E-01
Alkali burn	3	10	−0.077	8.33E-01

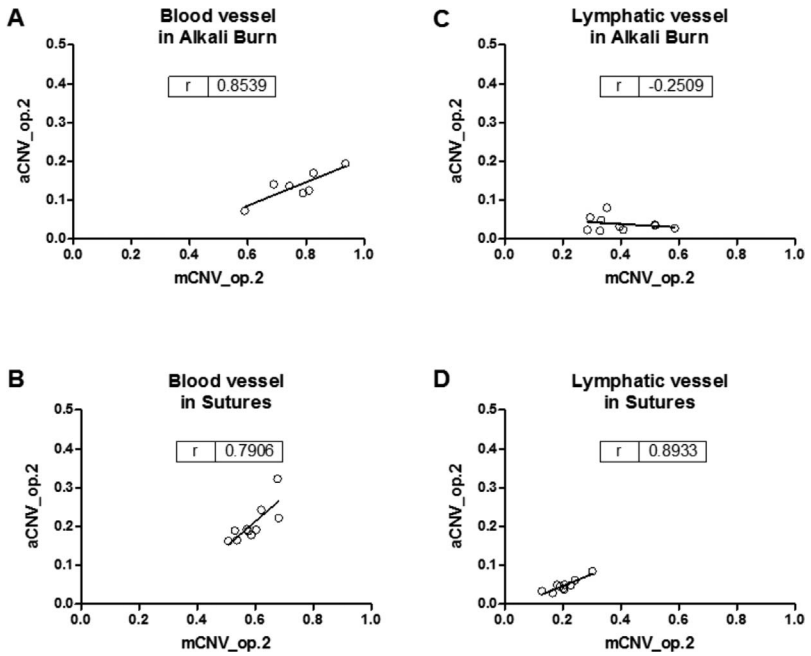

FIGURE 4. Representative correlation for operator 2 (op. 2) between manual corneal neovascularization (mCNV) and automatic corneal neovascularization (aCNV) for blood vessels in (**A**) alkali burn and (**B**) sutures models, and for lymphatic vessels in (**C**) alkali burn and (**D**) sutures models. *r*, Pearson correlation coefficient ($n = 7$–10).

tion, while manual lymphatic measure was more time-consuming compared to blood quantification. The time needed for manual quantification of lymphatic vessels was more than three times higher ($P < 0.01$) than for blood vessel quantification. This was probably due to the more uniform distribution of the blood vessel front. In summary, VesselJ is 21 and 6 times faster than the manual method for lymphatic and blood quantification, respectively.

Manual analysis of blood and lymphatic vessels in the sutures model was more time-consuming than in the alkali burn model, requiring approximately 30% more time. This was due to the less uniform distribution of the vessel front (data not shown); VesselJ, instead, processes all images in the same time (25.5 seconds).

DISCUSSION

In the present study, we describe a novel semiautomatic software (VesselJ) to objectively quantify corneal hem- and lymphangiogenesis in corneal flat mounts based on a stepwise color threshold algorithm. VesselJ proved to be extremely intuitive and user-friendly, allowing evaluation of corneal angiogenesis by almost anyone with no special training. We have developed VesselJ as an open-source plug-in for ImageJ; hence, it is free of charge. Additionally, it allows processing of multiple images at the same time and was demonstrated to be much faster than manual methods, which are generally used. The plug-in assigned a score between 0 and 1 for CNV, which is promptly exportable to an Excel spreadsheet. Since VesselJ does not graphically show which pixels have been counted as vessels or background, the user lacks direct feedback on false-positive or -negative results. However, the applied threshold value is provided in the result sheet. This value can be easily used to double-check the VesselJ analysis, if needed, with the method described in Supplementary Figure S4.

The VesselJ algorithm is based on a dynamic color threshold strategy, where the value is automatically set depending on the mean color intensity of background ROI area. Further, the computerized analysis does not depend on ROI size.

VesselJ cannot be properly defined as a fully automatic method, because operator's inputs are needed in the first few preliminary steps, specifically, choice of the marker stained (CD31 or LYVE1) and ROI placement in the background area. However, with the exception of these preparatory passages, VesselJ core allows automatic calculations of the threshold value and the corneal vessels. This strategy allowed us to overcome the major limit of the algorithm proposed by Bock et al.[13] Specifically, we removed the need to manually define a threshold number for each image, which in the prior method was required for the variability in background and staining intensity. Several advantages of automatic over semiautomatic methods have been elucidated, in particular better interrater reproducibility, less time to process a single image, and analysis of multiple images at once. This leaves the operator free to perform other activities.[20] In our VesselJ algorithm we chose to use a dynamic stepwise threshold, which can fit the background far better than a static one, whereas it generates less variability than a continuous scale.[21]

Background ROI selection is a crucial but operator-dependent step, so interrater variability and inaccuracy may

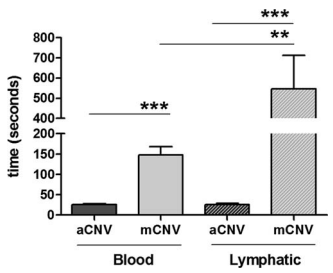

FIGURE 5. Time (in seconds) spent assessing manual corneal neovascularization (mCNV) and automatic corneal neovascularization (aCNV) for blood and lymphatic vessels in the alkali burn model. Histograms represent mean ± SD. $^{**}P < 0.01$; $^{***}P < 0.001$ ($n = 10$).

originate at this point. Moreover, the other potential source of interoperator variability is represented by the initial total corneal area selection. These are potential downsides of VesselJ. However, compared to the manual method, VesselJ improved the interrater reliability for both blood and lymphatic vessel quantification. Among blood vessels, reliability improved more in the sutures than in the alkali model. The most significant improvement, however, was noted for lymphatic vessels, especially in the sutures model where interrater reliability appeared to be unsatisfactory with the manual method. In addition, VesselJ showed an excellent intraoperator reproducibility as opposed to the manual method, which had a significant fluctuation over time for both vessel types.

Despite several studies that have applied some kind of semiautomatic morphometric analysis to quantify CNV, the comparison between VesselJ and such methods is not straightforward, because most studies do not detail the algorithm specifics, so it is not easy to understand how each method really works; and none of the studies (except for the one by Bock et al.[13]) performed an inter- or intraoperator reliability analysis.

Bock et al.[13] propose a semiautomatic algorithm for CNV quantification on corneal flat mounts. Their method, similarly to ours, has been validated in the sutures angiogenesis model. Bock's method, similarly to VesselJ, relies on an image binarization and CNV extraction. Despite the two methods showing a similar reliability, VesselJ exhibited a higher consistency for both vessel types and, above all, for lymphatics. These differences in consistency between the two methods can be explained considering that Bock's method required critical manual inputs (i.e., threshold value decision), and this could account for higher fluctuations at each measurement time point. Instead, manual inputs are reduced to a minimum in VesselJ, which could explain the very low fluctuation over time. Both methods provide a global CNV value as output, but no morphometric parameters, such as spatial allocation, tortuosity, and branching of vessels, as reported by Blacher et al.[22]

Grading scales have been applied in CNV quantification. They are generally ordinary scales arbitrarily assigned depending on the density, size, and tortuosity of the vessels.[5–8] Their greatest strength is that they are easy to use and low in cost. However, grading scales have several potential disadvantages compared to VesselJ, including the fact that they are extremely subjective, and thus they exhibit high intra- and interoperator variability.[23] Moreover, they are based on a semiquantitative scale, which is not as sensitive to detecting significant changes as a continuous one.[21]

A potential limit of the study is that a strong and significant correlation for all three operators between mCNV and aCNV was noted only for blood quantification in the sutures model. For the same model, a solid correlation for lymphatic vessels was significant only for operator 2. This could be explained by the fact that interrater reliability of mCNV was poor in this group and, thus, the operator exhibiting a significant correlation was probably the most accurate in manual analysis. We suggest that the lack of concordance between mCNV and aCNV observed in the alkali burn model for both blood and lymphatic vessels is imputable to limitations of the VesselJ algorithm. Quality of images obtained after alkali burn, however, was on average lower than after suture placement. This should be also taken into account when considering the limited reproducibility observed in this specific image set. Moreover, interrater variability in performing lymphatic manual analysis (ICC: 0.700, CI: 0.245–0.913) could also account for the lack of correlation between mCNV and aCNV in the alkali burn model.

The most notable limitation of VesselJ is the difficulty in determining the appropriate threshold value when the corneal background exhibits a fluorescence intensity similar to vessels (i.e., stromal autofluorescence, massive cell infiltration). In this case, VesselJ applied a threshold value too high or too low depending on whether the fluorescent background was included or not in the ROI. This condition was common in the alkali burn model, especially for lymphatic vessels analysis. Although sutured corneas numbered only 10, all of them had a clean background free from artifacts. This is in agreement with the fact that this model preserves tissue better than the alkali one. Thus, the quality of the staining is far better, with much fewer fluorescent artifacts.[11] We recommend checking for background quality prior to VesselJ launching in the alkali burn model. As a general rule, VesselJ can be applied to an image if the average color intensity of the weakest fluorescent vessels is at least double that of the most hyperfluorescent background area. Supplementary Figures S3 and S5 show examples of alkali-burned corneas that cannot or can be analyzed with VesselJ, respectively.

We suggest that VesselJ could be used also in other models of CNV (i.e., the micropocket assay) or, in general, other models of noncorneal angiogenesis. Since the micropocket assay generates a localized area of hyperfluorescence, which corresponds to the pellet implantation site, we would suggest manually removing (e.g., using a freehand selection) that area prior to VesselJ analysis. Notably, VesselJ was not validated for light wavelengths other than those used in this study (green and red light emissions).

In conclusion, in this study we developed an automated algorithm, named VesselJ. This is a reliable method to quantify corneal hem- and lymphangiogenesis in corneal flat mounts, specifically in the sutures model. It allowed us to automatically process multiple images at the same time in an automatic fashion. We suggest that VesselJ, which will be soon available free of charge (in the public domain, http://imagej.nih.gov/ij/plugins/index.html), may represent a helpful tool to quantify corneal angiogenesis, as the current gold standard (i.e., manual method) appeared to be less reproducible among raters. Since the corneal angiogenesis assay is widely used even in fields different from ophthalmology, such as oncology and wound healing, we suggest that VesselJ may represent a helpful tool also for researchers working in these areas.

Acknowledgments

Disclosure: **A. Rabiolo**, None; **F. Bignami**, None; **P. Rama**, None; **G. Ferrari**, None

References

1. Azar DT. Corneal angiogenic privilege: angiogenic and antiangiogenic factors in corneal avascularity, vasculogenesis, and wound healing (an American Ophthalmological Society thesis). *Trans Am Ophthalmol Soc*. 2006;104:264–302.
2. Chang JH, Gabison EE, Kato T, Azar DT. Corneal neovascularization. *Curr Opin Ophthalmol*. 2001;12:242–249.
3. Bock F, Maruyama K, Regenfuss B, et al. Novel anti(lymph)-angiogenic treatment strategies for corneal and ocular surface diseases. *Prog Retin Eye Res*. 2013;34:89–124.
4. Hos D, Schlereth SL, Bock F, Heindl LM, Cursiefen C. Antilymphangiogenic therapy to promote transplant survival and to reduce cancer metastasis: what can we learn from the eye? *Semin Cell Dev Biol*. 2015;38:117–130.
5. Chen L, Huq S, Gardner H, de Fougerolles AR, Barabino S, Dana MR. Very late antigen 1 blockade markedly promotes survival of corneal allografts. *Arch Ophthalmol*. 2007;125:783–788.
6. Lai LJ, Xiao X, Wu JH. Inhibition of corneal neovascularization with endostatin delivered by adeno-associated viral (AAV)

vector in a mouse corneal injury model. *J Biomed Sci*. 2007; 14:313–322.

7. Ling SQ, Liu C, Li WH, Xu JG, Kuang WH. Corneal lymphangiogenesis correlates closely with hemangiogenesis after keratoplasty. *Int J Ophthalmol*. 2010;3:76–79.
8. Zhang H, Grimaldo S, Yuen D, Chen L. Combined blockade of VEGFR-3 and VLA-1 markedly promotes high-risk corneal transplant survival. *Invest Ophthalmol Vis Sci*. 2011;52:6529–6535.
9. Bignami F, Giacomini C, Lorusso A, Aramini A, Rama P, Ferrari G. NK1 receptor antagonists as a new treatment for corneal neovascularization. *Invest Ophthalmol Vis Sci*. 2014;55:6783–6794.
10. Cho WK, Kang S, Choi H, Rho CR. Topically administered gold nanoparticles inhibit experimental corneal neovascularization in mice. *Cornea*. 2015;34:456–459.
11. Giacomini C, Ferrari G, Bignami F, Rama P. Alkali burn versus suture-induced corneal neovascularization in C57BL/6 mice: an overview of two common animal models of corneal neovascularization. *Exp Eye Res*. 2014;121:1–4.
12. Liclican EL, Nguyen V, Sullivan AB, Gronert K. Selective activation of the prostaglandin E2 circuit in chronic injury-induced pathologic angiogenesis. *Invest Ophthalmol Vis Sci*. 2010;51:6311–6320.
13. Bock F, Onderka J, Hos D, Horn F, Martus P, Cursiefen C. Improved semiautomatic method for morphometry of angiogenesis and lymphangiogenesis in corneal flatmounts. *Exp Eye Res*. 2008;87:462–470.
14. Chung ES, Chauhan SK, Jin Y, et al. Contribution of macrophages to angiogenesis induced by vascular endothelial growth factor receptor-3-specific ligands. *Am J Pathol*. 2009; 175:1984–1992.
15. Cursiefen C, Maruyama K, Bock F, et al. Thrombospondin 1 inhibits inflammatory lymphangiogenesis by CD36 ligation on monocytes. *J Exp Med*. 2011;208:1083–1092.
16. Lee H, Schlereth SL, Park EY, Emami-Naeini P, Chauhan SK, Dana R. A novel pro-angiogenic function for interferon-gamma-secreting natural killer cells. *Invest Ophthalmol Vis Sci*. 2014; 55:2885–2892.
17. Maruyama K, Nakazawa T, Cursiefen C, et al. The maintenance of lymphatic vessels in the cornea is dependent on the presence of macrophages. *Invest Ophthalmol Vis Sci*. 2012; 53:3145–3153.
18. Schroedl F, Kaser-Eichberger A, Schlereth SL, et al. Consensus statement on the immunohistochemical detection of ocular lymphatic vessels. *Invest Ophthalmol Vis Sci*. 2014;55:6440–6442.
19. Kottner J, Audige L, Brorson S, et al. Guidelines for Reporting Reliability and Agreement Studies (GRRAS) were proposed. *J Clin Epidemiol*. 2011;64:96–106.
20. Katouzian A, Angelini ED, Carlier SG, Suri JS, Navab N, Laine AF. A state-of-the-art review on segmentation algorithms in intravascular ultrasound (IVUS) images. *IEEE Trans Inf Technol Biomed*. 2012;16:823–834.
21. Bailey IL, Bullimore MA, Raasch TW, Taylor HR. Clinical grading and the effects of scaling. *Invest Ophthalmol Vis Sci*. 1991;32:422–432.
22. Blacher S, Detry B, Bruyere F, Foidart JM, Noel A. Additional parameters for the morphometry of angiogenesis and lymphangiogenesis in corneal flat mounts. *Exp Eye Res*. 2009;89: 274–276.
23. Chong E, Simpson T, Fonn D. The repeatability of discrete and continuous anterior segment grading scales. *Optom Vis Sci*. 2000;77:244–251.

Investigative Ophthalmology & Visual Science